micromachines

MDPI

*Article*

# Modeling and Simulation of Tin Sulfide (SnS)-Based Solar Cell Using ZnO as Transparent Conductive Oxide (TCO) and NiO as Hole Transport Layer (HTL)

**Ahmad Umar [1,2,*,†,‡], Pooja Tiwari [3,‡], Sadanand [4,*], Vaibhava Srivastava [3], Pooja Lohia [3], Dilip Kumar Dwivedi [5,*], Hussam Qasem [6], Sheikh Akbar [7], Hassan Algadi [7] and Sotirios Baskoutas [8]**

1 Department of Chemistry, College of Science and Arts, Promising Centre for Sensors and Electronic Devices (PCSED), Najran University, Najran 11001, Saudi Arabia
2 Department of Materials Science and Engineering, The Ohio State University, Columbus, OH 43210, USA
3 Department of Electronics and Communication Engineering, Madan Mohan Malviya University of Technology, Gorakhpur 273010, India
4 Department of Applied Sciences, Galgotias College of Engineering and Technology, Greater Noida 201306, India
5 Photonics and Photovoltaic Research Lab, Department of Physics and Material Science, Madan Mohan Malviya University of Technology, Gorakhpur 273010, India
6 National Centre for Renewable Energy, King Abdulaziz City for Science and Technology (KACST), Riyadh 11442, Saudi Arabia
7 Department of Electrical Engineering, College of Engineering, Najran University, Najran 11001, Saudi Arabia
8 Department of Materials Science, University of Patras, 26500 Patras, Greece
* Correspondence: ahmadumar786@gmail.com (A.U.); sadanand2893@gmail.com (S.); todkdwivedi@gmail.com (D.K.D.)
† Adjunct Professor at the Department of Materials Science and Engineering, The Ohio State University, Columbus, OH 43210, USA.
‡ These authors contributed equally to this work.

check for updates

**Citation:** Umar, A.; Tiwari, P.; Sadanand; Srivastava, V.; Lohia, P.; Dwivedi, D.K.; Qasem, H.; Akbar, S.; Algadi, H.; Baskoutas, S. Modeling and Simulation of Tin Sulfide (SnS)-Based Solar Cell Using ZnO as Transparent Conductive Oxide (TCO) and NiO as Hole Transport Layer (HTL). *Micromachines* **2022**, *13*, 2073. https://doi.org/10.3390/mi13122073

Academic Editor: Jinn-Kong Sheu

Received: 20 October 2022
Accepted: 22 November 2022
Published: 25 November 2022

**Publisher's Note:** MDPI stays neutral with regard to jurisdictional claims in published maps and institutional affiliations.

**Copyright:** © 2022 by the authors. Licensee MDPI, Basel, Switzerland. This article is an open access article distributed under the terms and conditions of the Creative Commons Attribution (CC BY) license (https://creativecommons.org/licenses/by/4.0/).

**Abstract:** This paper describes the simulation by Solar Cell Capacitance Simulator-1D (SCAPS-1D) software of ZnO/CdS/SnS/NiO/Au solar cells, in which zinc oxide (ZnO) is used as transparent conductive oxide (TCO) and nickel oxide (NiO) is used as a hole transport layer (HTL). The effects of absorber layer (SnS) thickness, carrier concentration, SnS defect density, NiO HTL, ZnO TCO, electron affinity and work function on cell performance have been evaluated. The effect of interface defect density of SnS/CdS on the performance of the heterojunction solar cell is also analysed. As the results indicate, a maximum power conversion efficiency of 26.92% was obtained.

**Keywords:** SnS; heterojunction solar cell; CdS

## 1. Introduction

Global energy consumption is rising as a result of population growth and a wide use of digital substances in practically every aspect of our lives. The major source of energy is fossil fuels [1] which is not a long-term energy source. The burning of fossil fuels emits a large amount of carbon dioxide [2]. Furthermore, fossil fuels are not a sustainable source. For these reasons, the energy sector is expanding but shifting to sustainable sources of energy as the optimum choice. Solar cells can be a viable substitute for fossil fuels. Many researchers have recently concentrated on highly efficient polymer and perovskite cells [3,4], but these solar cells suffer from instability which limits their long-term application areas. As a result, the thin-film solar cell may be used in place of polymer and perovskite solar cells.

Tin monosulphide (SnS) has been developed as a significant absorbent layer in thin-film solar cells having various advantages such as a high absorption coefficient that allows SnS to absorb a considerable portion of the spectrum. SnS is an Earth-abundant material which can be manufactured at low cost [5–9]. The energy gap at the absorber and back

contact interface has a significant impact on the performance of the cell. This energy gap can be reduced by using a small resistive back contact with higher work function (WF). High WF transition metal oxides (TMOs) such as $MoO_X$ [10–12], $V_2O_5$ [13], NiO [14] and $WO_3$ [15] were used as HTLs in several solar cells for performance improvement. NiO is a highly useful HTL within all TMOs due to its wide bandgap (3.5–3.8 eV) and high WF (5 eV). Polycrystalline CdS is used as a window layer, having many features such as high absorption coefficient, electron affinity, low resistivity, high optical transmittance, wide bandgap and good electrical properties that are suitable for solar cell fabrication and applications as well. TCO in a solar cell is usually indium tin oxide (ITO) or fluorine-doped tin oxide (FTO) which are quite expensive, and ITO has stability limitations. ZnO is used as TCO, having a wide bandgap of 3.37 eV, excellent electrical and optical properties, and it is Earth abundant [16,17]. Furthermore, different parameters such as carrier concentration, SnS layer thickness and defects have a considerable impact on the performance of the cell [18–21].

In this study, a new highly efficient structure of ZnO/CdS/SnS/NiO/Au of SnS-based solar cells is designed. SCAPS 1-D software is used to perform a numerical study of the developed cell. The influence of various parameters of ZnO, SnS and NiO HTL on the performance of the solar cell has been studied. The improved solar cell achieved a maximum efficiency of 26.92%.

## 2. Modelling and Simulation

Simulation software of solar cells is designed to solve semiconductor material property equations. SCAPS 1-D software is much more popular than other simulation software due to its ability to simulate up to seven layers of structure [22,23]. SCAPS 1-D simulator is used in the modelling of ZnO/CdS/SnS/NiO/Au heterostructure cells. It includes the following equations for measurements of J-V, C-V, C-F properties and quantum efficiency of the solar cell.

$$\text{Poisson's equation: } (\partial^2 \Psi/\partial x^2) + (q/\varepsilon)\,[\,p(x) - n(x) + N_D - N_A + \rho_p - \rho_n = 0, \quad (1)$$

$$\text{Hole continuity equation: } (1/q)\,(\partial J_p/\partial x) = G_{op} - R(x), \quad (2)$$

$$\text{Electron continuity equation: } (1/q)\,(\partial Jn/\partial x) = -Gop + R(x), \quad (3)$$

where $\varepsilon$ = dielectric constant, q = charge of the electron, $N_A$ = acceptor density, $N_D$ = donor density, $\Psi$ = electrostatic potential, Jp = current density due to holes, Jn = current density due to electrons, $G_{op}$ = carrier generation rate, R = total recombination rate, $\rho_p$ and $\rho_n$ = hole and electron distribution, respectively.

The semiconducting material's holes and electron charge carrier characteristics are represented by the drift and diffusion equations [24] given below:

$$J_p = -(\mu_p\, p)/q\,(\partial E_{Fp}/\partial x), \quad (4)$$

$$J_n = -(\mu_n\, n)/q\,(\partial E_{Fn}/\partial x), \quad (5)$$

where $\mu_p$ and $\mu_n$ = holes and electron mobility, respectively, $E_{Fp}$ and $E_{Fn}$ = p-type and n-type fermi level, respectively.

## 3. Solar Cell Structure and Material Properties

The schematic structure and energy band diagram of the proposed ZnO/CdS/SnS/NiO/Au cell are shown In Figure 1a,b with ZnO serving as TCO, CdS as the window layer, SnS as the absorber layer, NiO as HTL and Au as back metal contact. ZnO is an n-type semiconductor used as the substitute of ITO and FTO because of its excellent electrical and optical properties. Figure 1b shows that the conduction band of SnS is smaller than that of CdS and the conduction band offset (CBO) between them is also very low. Thus, electrons can flow easily from SnS to ZnO through CdS. The valence band of NiO is higher

than that of SnS and the valence band offset (VBO) between them is smaller. Furthermore, CBO between SnS and NiO is relatively high, stopping electrons from entering the back electrode. For benchmarking purposes, we have used a ZnO/CdS/CdTe/SnS/Ni device structure [25]. The physical parameters used in the modelling of ZnO/CdS/SnS/NiO are stated in Table 1 and interface parameters of SnS/CdS are listed in Table 2.

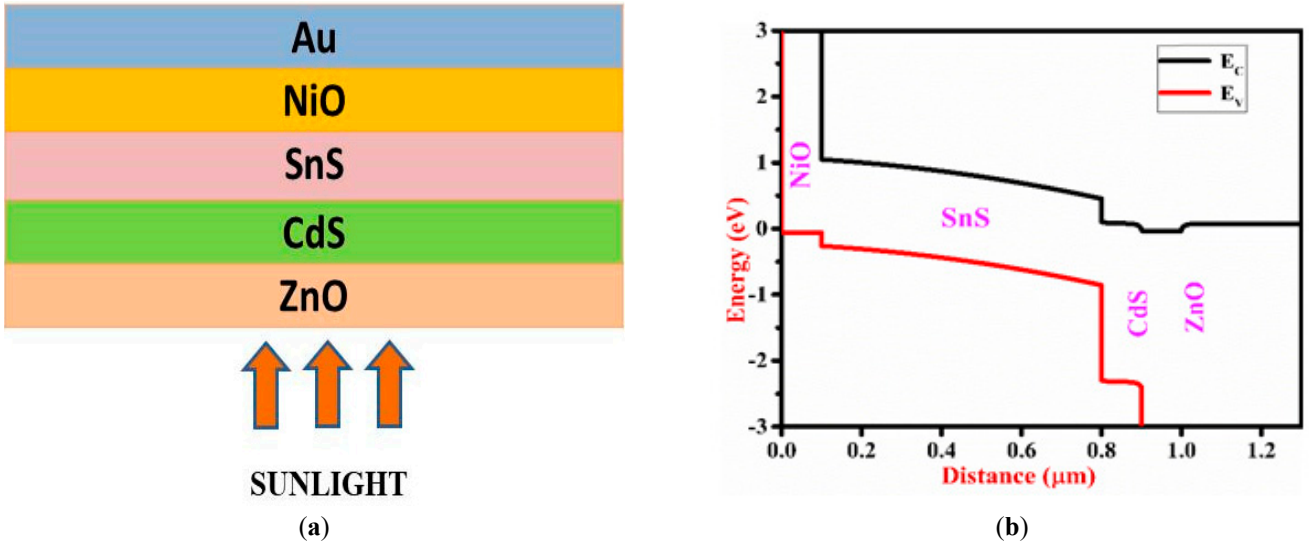



**Figure 1.** (**a**) Schematic structure and (**b**) energy band diagram of the proposed solar cell.

**Table 1.** Parameters of ZnO [26], CdS [27], SnS [28] and NiO [14] used in the simulation of proposed solar cell.

| Parameters | ZnO | CdS | SnS | NiO |
|---|---|---|---|---|
| Thickness (nm) | 100 | 100 | 1000 | 250 |
| Bandgap (eV) | 3.37 | 2.4 | 1.31 | 3.8 |
| Electron affinity (eV) | 4.5 | 4.5 | 4.3 | 1.46 |
| Dielectric permittivity (relative) | 9 | 10 | 13 | 10 |
| CB effective density of states ($cm^{-3}$) | $2.2 \times 10^{18}$ | $2.2 \times 10^{18}$ | $1.18 \times 10^{18}$ | $2.8 \times 10^{19}$ |
| VB effective density of states ($cm^{-3}$) | $1.8 \times 10^{18}$ | $1.9 \times 10^{19}$ | $4.76 \times 10^{18}$ | $1 \times 10^{18}$ |
| Electron mobility ($cm^2/V_S$) | 100 | 350 | 130 | 12 |
| Hole mobility ($cm^2/V_S$) | 25 | 25 | 4.3 | 2.8 |
| Shallow uniform donor density $N_d$ ($cm^{-3}$) | $1 \times 10^{17}$ | $1 \times 10^{17}$ | $1 \times 10^{7}$ | 0 |
| Shallow uniform acceptor density $N_a$ ($cm^{-3}$) | 0 | 0 | $1 \times 10^{15}$ | $1 \times 10^{21}$ |
| Electron thermal velocity (cm/s) | $1 \times 10^{7}$ | $1 \times 10^{7}$ | $1 \times 10^{7}$ | $1 \times 10^{7}$ |
| Hole thermal velocity (cm/s) | $1 \times 10^{7}$ | $1 \times 10^{7}$ | $1 \times 10^{7}$ | $1 \times 10^{7}$ |
| Defect density ($cm^{-3}$) | $1 \times 10^{14}$ | $1 \times 10^{14}$ | $1 \times 10^{11}$ | $1 \times 10^{14}$ |
| Radiative recombination coefficient ($cm^3/s$) | $2.3 \times 10^{-9}$ | $2.3 \times 10^{-9}$ | $2.3 \times 10^{-9}$ | $2.3 \times 10^{-9}$ |
| Absorption coefficient ($cm^{-1}$) | SCAPS | $1 \times 10^{5}$ | $1 \times 10^{5}$ | $1 \times 10^{5}$ |

**Table 2.** Interface parameters used in the simulation of the proposed solar cell.

| Parameters | SnS/CdS Interface [28] |
|---|---|
| Defect type | Neutral |
| Capture cross-section electrons ($cm^2$) | $1 \times 10^{-19}$ |
| Capture cross-section holes ($cm^2$) | $1 \times 10^{-19}$ |
| Defect energy level $E_t$ | Above the highest $E_v$ |
| Energy with respect to a reference (eV) | 0.06 |
| Total density ($cm^{-2}$) | $1 \times 10^{10}$ |

## 4. Results and Discussion

The heterostructure ZnO/CdS/SnS solar cells have $V_{OC}$, $J_{SC}$, FF and PCE of 0.4732 V, 33.739 mA/$cm^2$, 71.79% and 11.46%, respectively. Figure 2a,b display the J-V characteristics and quantum efficiency (QE) of the heterostructure ZnO/CdS/SnS/NiO/Au solar cell. The improved solar cell achieved $V_{OC}$, $J_{SC}$, FF and PCE of 0.9048 V, 34.209 mA/$cm^2$, 86.97% and 26.92%, respectively. After including NiO and other materials, the QE of the solar cell increases from the wavelength of 600-900 nm as shown in Figure 2(b). This enhancement of QE shows the reduction in surface carrier recombination at SnS that demonstrated the improvement of PCE after employing NiO as the HTL. The PCE of the enhanced cell is increased below the wavelength of 400 nm.

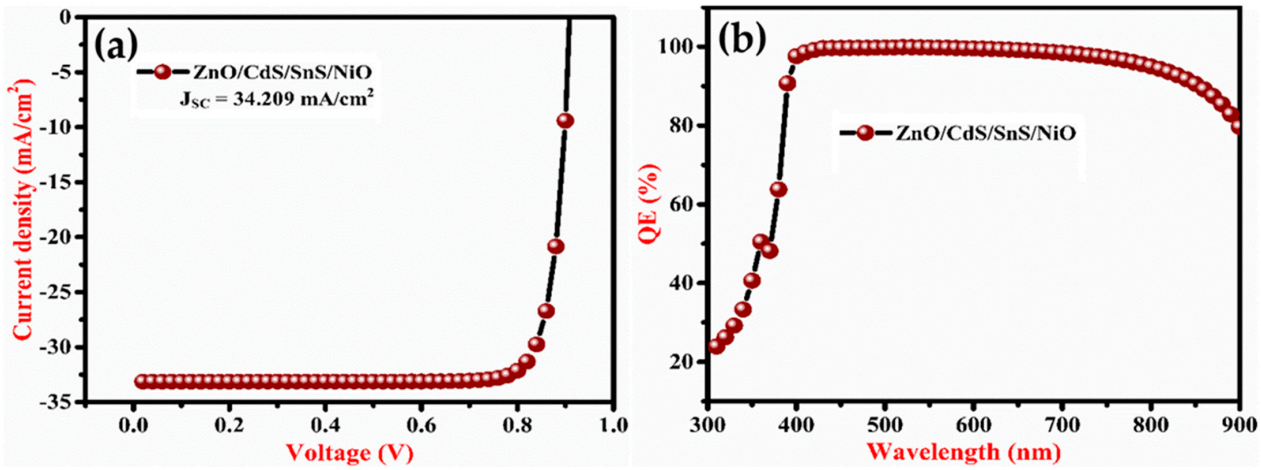



**Figure 2.** (**a**) J-V curve and (**b**) quantum efficiency of the proposed heterojunction solar cell.

### *4.1. Impact of Carrier Concentration and Thickness of NiO and ZnO*

The cell performance was studied in terms of carrier concentration and layer thickness. The thickness of NiO and ZnO was varied from 100 to 12,000 nm and carrier concentration was varied from $10^{14}$ to $10^{21}$ $cm^{-3}$. The $V_{OC}$ is nearly independent of both carrier concentration and NiO thickness. The $J_{SC}$ varies significantly depending on carrier concentration and thickness. At a NiO carrier concentration of $10^{18}$ $cm^{-3}$ and thickness of 250 nm, the optimal $J_{SC}$ of 34.20 mA/$cm^2$ was obtained. The FF and PCE increase with an increase in carrier concentration but remain almost constant with increasing thickness. The series resistance decreases as the carrier concentration increases due to which FF and PCE rise [10]. At a NiO carrier concentration of $10^{21}$ $cm^{-3}$ and thickness of 250 nm, the maximum PCE of 26.92% is recorded.

The thickness of ZnO does not have any effect on $V_{OC}$ but fluctuates with carrier concentration and achieves its maximum value of 0.9048 V at $10^{17}$ $cm^{-3}$. The $J_{SC}$ worked similarly to the $V_{OC}$ and gave an optimal value of $J_{SC}$ 34.20 mA/$cm^2$ at $10^{17}$ $cm^{-3}$ carrier concentration. The increase in ZnO carrier concentration induced band bending resulting

in a small rise in $J_{SC}$. The FF had a reducing nature with increasing thickness of ZnO up to $10^{17}$ $cm^{-3}$ because of increasing series resistance. Maximum efficiency of 26.92% is recorded at carrier concentration and thickness of $10^{17}$ $cm^{-3}$ and 100 nm, respectively.

### *4.2. Impact of SnS/CdS Interface Defect Density*

The influences of SnS/CdS interface defect density (IDD) on the performance of the proposed solar cell have been analysed. The SnS/CdS defect interface can increase the series resistance and carrier trapping of the cell. Due to the increase in carrier recombination rate at the interface, $V_{OC}$ decreases with IDD but IDD has no impact on $J_{SC}$ until $10^{17}$ $cm^2$. $J_{SC}$ increases from 19.48 to 28.25 $mA/cm^2$ when the width of SnS layer increases from 200 to 1200 nm. When IDD increases from $10^{11}$ to $10^{18}$ $cm^2$, FF decreases rapidly from 84.9% to 54.8% due to an increase in the series resistance of the cell, indicating that high defect density at SnS/CdS is responsible for high series resistance. A significant decrease in PCE was also seen with increasing IDD. An interface defect is one of the reasons for lower PCE. Defects in the interfacial layer density are induced in the cell as a result of structural changes in the materials produced during the fabrication process.

### *4.3. Impact of Defect Density and Thickness of Absorber Layer SnS*

The influence of absorber layer defect density and thickness is depicted in Figures 3 and 4, respectively. The defect is caused by displacement and surface defects. Defects serve in carrier recombination, reducing mobility and carrier lifetime. The Shockley–Read–Hall (SRH) process modulates the recombination rate of SnS at higher defect density.

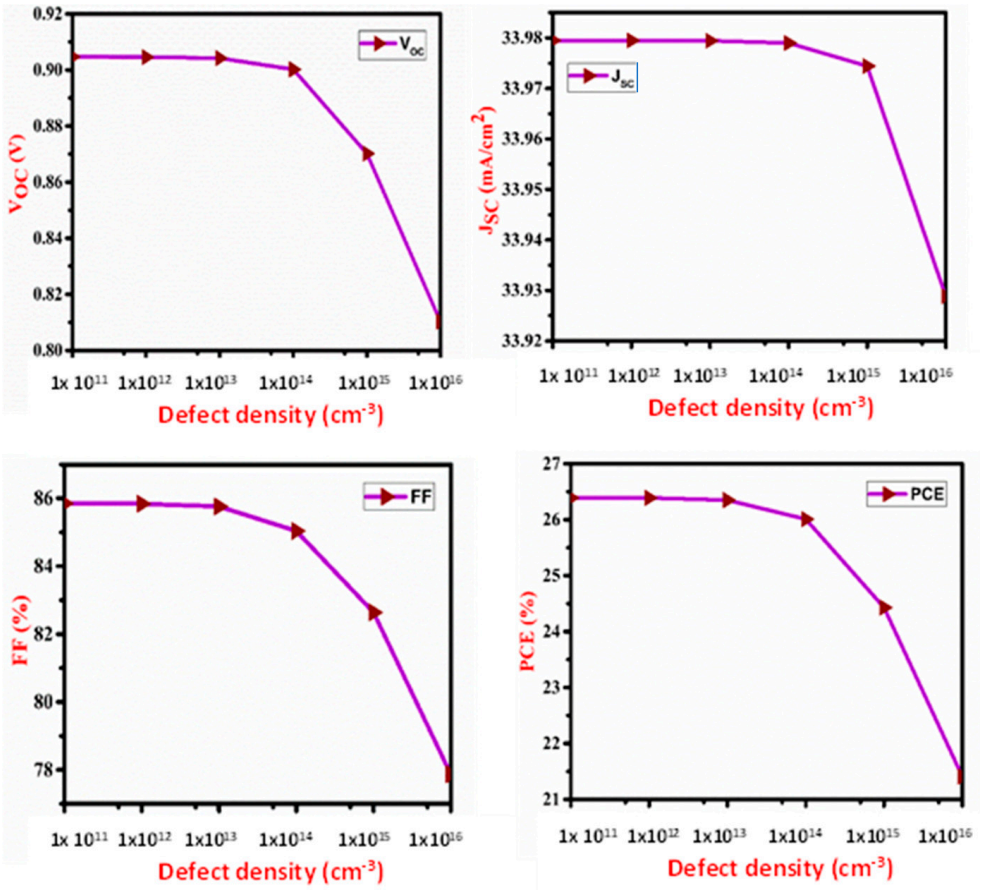



**Figure 3.** Impact of defect density of SnS layer on $V_{OC}$, $J_{SC}$, FF and PCE of the proposed cell.

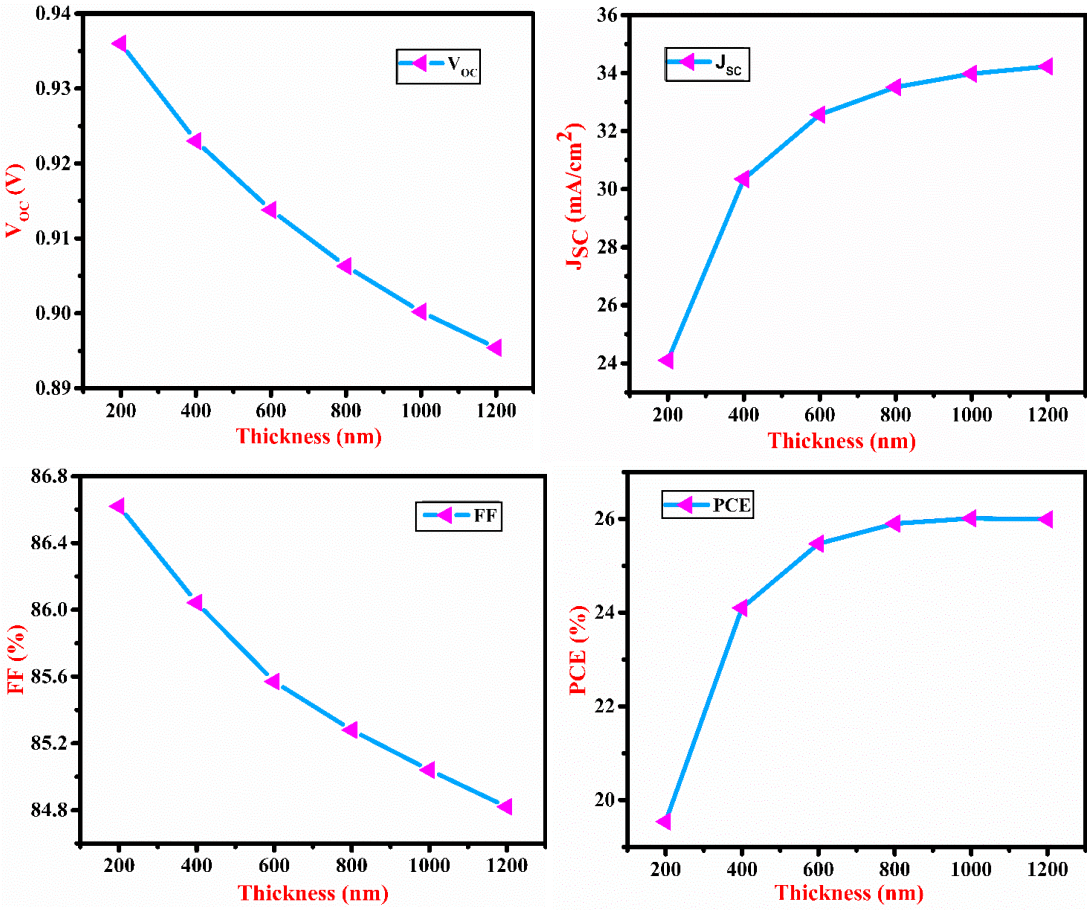



**Figure 4.** Impact of SnS layer thickness on $V_{OC}$, $J_{SC}$, FF and PCE of the proposed cell.

The absorber layer thickness and defect density varied from 100 to 1200 nm and from $10^{11}$ to $10^{16}$ $cm^{-3}$, respectively. $V_{OC}$ decreases with an increase in thickness and defect density of SnS but there is no effect of defect density on $J_{SC}$ below $10^{15}$ $cm^{-3}$ due to an increase in carrier recombination. Due to the high absorption of increased wavelength photons in the layer, $J_{SC}$ increases up to a certain level with an increase in the thickness of SnS. After that, it saturates due to light absorption saturation. PCE is increased with SnS thickness as the $J_{SC}$ increases and saturates at 1200 nm due to the light absorption saturation. The fill factor shows the same nature as $V_{OC}$. $J_{SC}$, $V_{OC}$ and FF are all associated with PCE. At defect density of $10^{11}$ $cm^{-3}$ and thickness of the SnS layer of 1000 nm, the maximum PCE of 26.92% is recorded.

### *4.4. Impact of Electron Affinity and Back Contact Metal Work Function of Absorber Layer SnS*

Figure 5 depicts the effect of SnS electron affinity (EA). The maximum performance of the cell was obtained at SnS EA of 4.3 eV. Due to a decrease in FF, PCE falls with EA > 4.3 eV due to a mismatch of energy level between the SnS and CdS layer for electron transport as shown in Figure 5. $V_{OC}$ does not show any significant change with affinity due to insufficient carriers. The effect of back contact metal work function (WF) is shown in Figure 6. As the WF increases, $J_{SC}$, $V_{OC}$, FF and PCE also increase up to a certain WF level. This indicates that when WF rises, the majority carrier barrier height reduces. As a result, PCE rises with WF till 5 eV, and after 5 eV, PCE saturates. Thus, WF has a significant influence on the performance of the solar cell. Proper metal contact is necessary to achieve high efficiency. Table 3 shows a comparison of the physical parameters of various simulated device structures. Our findings seem to have a satisfying consistency with those that have already been published.

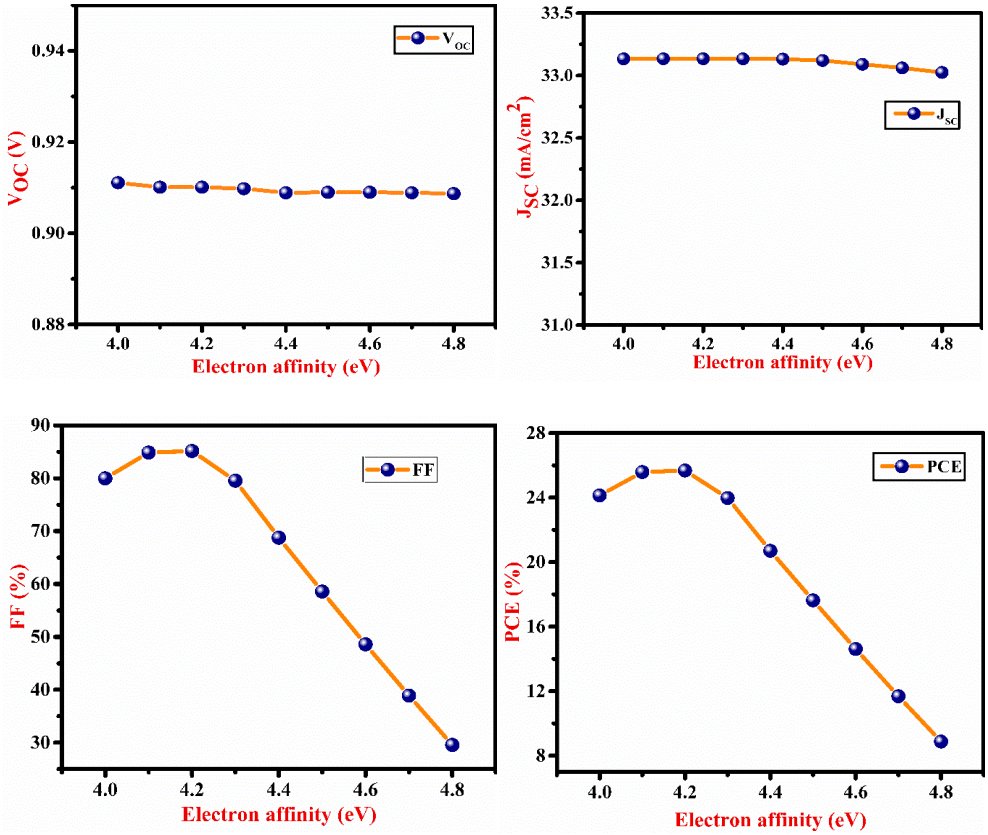



**Figure 5.** Impact of the electron affinity of SnS layer on $V_{OC}$, $J_{SC}$, FF and PCE of the proposed cell.

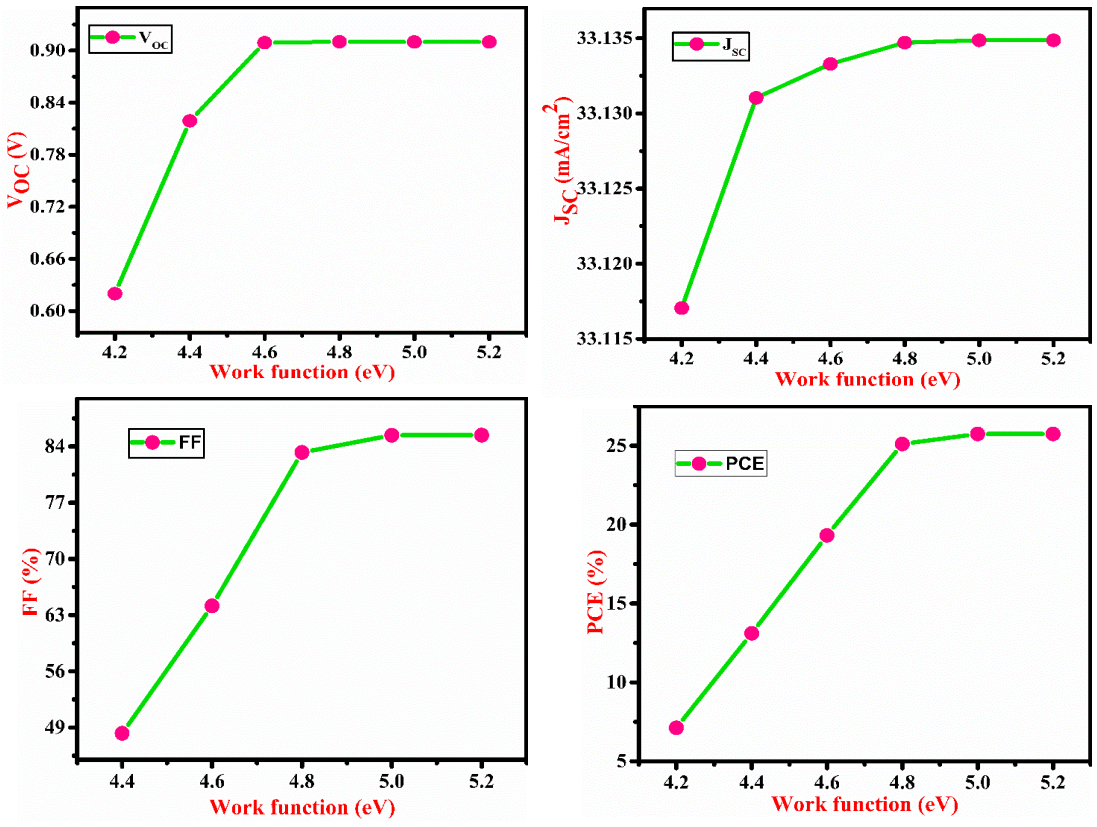



**Figure 6.** Impact of back contact metal work function on $V_{OC}$, $J_{SC}$, FF and PCE of the proposed cell.

**Table 3.** Comparison of previously reported results to proposed work.

| Structures | $V_{OC}$ V | $J_{SC}$ mA/cm$^2$ | FF % | PCE % | References |
|---|---|---|---|---|---|
| ITO/$CeO_2$/SnS/NiO/Mo (simulated ITO) | 0.890 | 32.67 | 86.19 | 25.06 | [14] |
| ITO/$CeO_2$/SnS/Spiro-OMeTAD (simulated) | 0.887 | 33.74 | 85.61 | 25.65 | [28] |
| p-SnS/CdS/n-Zn MgO (simulated) | ~0.7 | 38.54 | 83 | ~23 | [29] |
| ZnO/CdS/SnS (simulated) | 0.73 | 33.20 | 61.47 | 14.9% | [30] |
| ZnO/CdS/CdTe/SnS/Ni (simulated) | 0.845 | 26.46 | 84.50 | 21.83 | [24] |
| ZnO/CdS/SnS/NiO (simulated) | 0.904 | 34.20 | 86.97 | 26.92 | This paper |

## 5. Conclusions

The performance of the cell structure ZnO/CdS/SnS/NiO/Au has been investigated using SCAPS 1-D software. It is shown that NiO is a suitable HTL material with the ability to improve the efficiency of SnS-based solar cells. ZnO can be a good replacement for ITO and FTO in the fabrication of low-cost and highly efficient SnS-based solar cells. At ZnO and NiO carrier concentrations of $10^{17}$ and $10^{21}$ cm$^{-3}$, respectively, and thicknesses of 100 and 250 nm, respectively, the maximum PCE of 26.92% is recorded. The thickness and defect density of the SnS layer were also investigated. As the SnS thickness increases, the PCE of the cell also increases. The maximum PCE of the proposed solar cell is recorded at thickness and defect density of 1000 nm and $10^{11}$ cm$^{-3}$. The present work might give an insight into the modelling and development of the high performance of SnS-based solar cells.

**Author Contributions:** Conceptualization, A.U., P.T., S., P.L. and D.K.D.; methodology, A.U., P.T., S., P.L. and D.K.D.; software, A.U., P.T., S., V.S., P.L., D.K.D. and H.Q.; validation, A.U., P.T., S., V.S., P.L., D.K.D., H.Q., S.A., H.A. and S.B.; formal analysis, A.U., P.T., S., V.S., P.L., D.K.D., H.Q., S.A., H.A. and S.B.; resources, A.U. and D.K.D.; data curation, A.U., P.T., S., V.S., P.L., D.K.D., H.Q., S.A., H.A. and S.B.; writing—original draft preparation, A.U., P.T., S. and D.K.D.; writing—review and editing, A.U., S., D.K.D., H.Q., S.A. and S.B.; supervision, A.U., S. and D.K.D.; project administration, A.U. and D.K.D.; funding acquisition, A.U. All authors have read and agreed to the published version of the manuscript.

**Funding:** The authors are thankful to the Deanship of Scientific Research at Najran University, Najran, Kingdom of Saudi Arabia, for funding this work under the Research Group Funding Program grant NU/RG/SERC/11/1.

**Data Availability Statement:** All data is provided in the manuscript.

**Acknowledgments:** The authors are thankful to the Deanship of Scientific Research at Najran University, Najran, Kingdom of Saudi Arabia, for funding this work under the Research Group Funding Program grant NU/RG/SERC/11/1. The authors also thank Mark Burgelman for developing the SCAPS-1D software and making it freely accessible to the entire scientific community.

**Conflicts of Interest:** The authors declared no potential conflict of interest.

## References


1. Andrade-Arvizu, J.A.; Courel-Piedrahita, M.; Vigil-Galán, O. SnS-based thin film solar cells: Perspectives over the last 25 years. *J. Mater. Sci. Mater. Electron.* **2015**, *26*, 4541–4556. [CrossRef]
2. Hammond, G.P.; Pearson, P.J. Challenges of the transition to a low carbon, more electric future: From here to 2050. *Energy Policy* **2013**, *52*, 1–9. [CrossRef]
3. Huang, J.; Xiang, S.; Yu, J.; Li, C.-Z. Highly efficient prismatic perovskite solar cells. *Energy Environ. Sci.* **2018**, *12*, 929–937. [CrossRef]
4. Wang, C.; Liu, M.; Rahman, S.; Pasanen, H.P.; Tian, J.; Li, J.; Deng, Z.; Zhang, H.; Vivo, P. Hydrogen bonding drives the self-assembling of carbazole-based hole-transport material for enhanced efficiency and stability of perovskite solar cells. *Nano Energy* **2022**, *101*, 107604. [CrossRef]
5. Li, R.; Liu, M.; Matta, S.K.; Hiltunen, A.; Deng, Z.; Wang, C.; Dai, Z.; Russo, S.P.; Vivo, P.; Zhang, H. Sulfonated Dopant-Free Hole-Transport Material Promotes Interfacial Charge Transfer Dynamics for Highly Stable Perovskite Solar Cells. *Adv. Sustain. Syst.* **2021**, *5*, 2100244. [CrossRef]
6. Patel, M.; Mukhopadhyay, I.; Ray, A. Molar optimization of spray pyrolyzed SnS thin films for photoelectrochemical applications. *J. Alloys Compd.* **2015**, *619*, 458–463. [CrossRef]
7. Tumen-Ulzii, G.; Matsushima, T.; Adachi, C. Mini-Review on Efficiency and Stability of Perovskite Solar Cells with Spiro-OMeTAD Hole Transport Layer: Recent Progress and Perspectives. *Energy Fuels* **2021**, *35*, 18915–18927. [CrossRef]
8. Devika, M.; Reddy, N.K.; Ramesh, K.; Patolsky, F.; Gunasekhar, K. Weak rectifying behaviour of p-SnS/n-ITO heterojunctions. *Solid-State Electron.* **2009**, *53*, 630–634. [CrossRef]
9. Jeganath, K.; Choudhari, N.J.; Pai, G.S.; Rao, A.; Raviprakash, Y. Role of substrate temperature on spray pyrolysed metastable π-SnS thin films. *Mater. Sci. Semicond. Process.* **2020**, *113*, 105050. [CrossRef]
10. Yang, R.; Wang, D.; Jeng, M.; Ho, K.; Wang, D. Stable CdTe thin fi lm solar cells with a MoO x back- contact buffer layer. *Prog. Photovolt. Res. Appl.* **2016**, *24*, 59–65. [CrossRef]
11. Irfan, I.; Lin, H.; Xia, W.; Wu, H.N.; Tang, C.W.; Gao, Y. The effect of MoOx inter-layer on thin film CdTe/CdS solar cell. *Sol. Energy Mater. Sol. Cells* **2012**, *105*, 86–89. [CrossRef]
12. Lin, H.; Irfan, H.; Xia, W.; Wu, H.N.; Gao, Y.; Tang, C.W. MoOx back contact for CdS/CdTe thin film solar cells: Preparation, device characteristics, and stability. *Sol. Energy Mater. Sol. Cells* **2012**, *99*, 349–355. [CrossRef]
13. Shen, K.; Yang, R.; Wang, D.; Jeng, M.; Chaudhary, S.; Ho, K.; Wang, D. Stable CdTe solar cell with V2O5 as a back contact buffer layer. *Sol. Energy Mater. Sol. Cells* **2016**, *144*, 500–508. [CrossRef]
14. Ahmmed, S.; Aktar, A.; Hossain, J.; Ismail, A.B.M. Enhancing the open circuit voltage of the SnS based heterojunction solar cell using NiO HTL. *Sol. Energy* **2020**, *207*, 693–702. [CrossRef]
15. Kazemzadeh, M.; Ranjbar, M.; Kermanpur, A.; Taghaviniaet, N.; Minbashi, M.; Forouzandeh, M.; Ebadi, F. Enhanced performance of planar perovskite solar cells using $TiO_2/SnO_2$ and $TiO_2/WO_3$ bilayer structures: Roles of the interfacial layers. *Sol. Energy* **2020**, *208*, 697–707.
16. Agrawal, S.; Rane, R.; Mukherjee, S. ZnO Thin Film Deposition for TCO Application in Solar Cell. *Conf. Pap. Energy* **2013**, *2013*, 718692. [CrossRef]
17. Muchuweni, E.; Sathiaraj, T.; Nyakotyo, H. Synthesis and characterization of zinc oxide thin films for optoelectronic applications. *Heliyon* **2017**, *3*, e00285. [CrossRef]
18. Wang, K.-C.; Jeng, J.-Y.; Shen, P.-S.; Chang, Y.-C.; Diau, E.W.-G.; Tsai, C.-H.; Chao, T.-Y.; Hsu, H.-C.; Lin, P.-Y.; Chen, P.; et al. p-type Mesoscopic Nickel Oxide/Organometallic Perovskite Heterojunction Solar Cells. *Sci. Rep.* **2014**, *4*, 4756. [CrossRef]
19. Reese, M.O.; Barnes, T.M.; Jensen, S.A.; Metzger, W.K. The Roles of Carrier Concentration and Interface, Bulk, and Grain-Boundary Recombination for 25% Efficient CdTe Solar Cells. *J. Appl. Phys.* **2017**, *121*, 214506.
20. Nayak, P.K.; Mahesh, S.; Snaith, H.J.; Cahen, D. Photovoltaic solar cell technologies: Analysing the state of the art. *Nat. Rev. Mater.* **2019**, *4*, 269–285. [CrossRef]
21. Kavitha, N.; Chandramohan, R.; Valanarasu, S.; Vijayan, T.A.; Rosario, S.R.; Kathalingam, A. Effect of film thickness on the solar cell performance of CBD grown CdS/PbS heterostructure. *J. Mater. Sci. Mater. Electron.* **2015**, *27*, 2574–2580. [CrossRef]
22. Alam Moon, M.; Ali, H.; Rahman, F.; Hossain, J.; Ismail, A.B. Design and Simulation of $FeSi_2$-Based Novel Heterojunction Solar Cells for Harnessing Visible and Near-Infrared Light. *Phys. Status solidi* **2020**, *217*, 1900921. [CrossRef]
23. Et-Taya, L.; Ouslimane, T.; Benami, A. Numerical analysis of earth-abundant Cu2ZnSn(SxSe1-x)4 solar cells based on Spectroscopic Ellipsometry results by using SCAPS-1D. *Sol. Energy* **2020**, *201*, 827–835. [CrossRef]
24. Procel, P.; Xu, H.; Saez, A.; Ruiz-Tobon, C.; Mazzarella, L.; Zhao, Y.; Han, C.; Yang, G.; Zeman, M.; Isabella, O. The role of heterointerfaces and subgap energy states on transport mechanisms in silicon heterojunction solar cells. *Prog. Photovolt. Res. Appl.* **2020**, *28*, 935–945. [CrossRef]
25. Benabbasa, S.; Rouabaha, Z.; Bouarissab, N.; Chelalia, N. The role of back surface field SnS layer in improvement of efficiency of CdTe thin film solar cells. *Optik* **2016**, *127*, 6210–6217. [CrossRef]
26. Boudour, S.; Bouchama, I.; Hadjab, M.; Laidoudi, S. Optimization of defected ZnO/Si/Cu2O heterostructure solar cell. *Opt. Mater.* **2019**, *98*, 109433. [CrossRef]
27. Nykyruy, L.; Yavorskyi, R.; Zapukhlyak, Z.; Wisz, G.; Potera, P. Evaluation of CdS/CdTe thin film solar cells: SCAPS thickness simulation and analysis of optical properties. *Opt. Mater.* **2019**, *92*, 319–329. [CrossRef]

28. Tiwari, P.; Alotaibi, M.F.; Al-Hadeethi, Y.; Srivastava, V.; Arkook, B.; Sadanand, S.; Lohia, P.; Dwivedi, D.K.; Umar, A.; Algadi, H.; et al. Design and Simulation of Efficient SnS-Based Solar Cell Using Spiro-OMeTAD as Hole Transport Layer. *Nanomaterials* **2022**, *12*, 2506. [CrossRef]
29. Kutwade, V.V.; Gattu, K.P.; Sonawane, M.E.; Tonpe, D.A.; Mishra, M.K.; Sharma, R. Contribution in PCE enhancement: Numerical designing and optimization of SnS thin film solar cell. *J. Nanopart. Res.* **2021**, *23*, 146. [CrossRef]
30. Boubakri, A.; Jouidri, A.; Koumya, Y.; Rajira, A.; Almaggoussi, A.; Abounadi, A. An output characteristics simulation of SnS based solar cells. *Mater. Today Proc.* **2021**, *51*, 2047–2052. [CrossRef]